Time Resolved Microscopic Analysis of Ink Layer Surface in Laser Dye Thermal Transfer Printing

Masaru Kinoshita*,‡,▲, Katsuyoshi Hoshino*,†, and Takashi Kitamura*,†,▲

*Graduate School of Science and Technology, Chiba University, Japan

†Information and Image Sciences Department, Faculty of Engineering, Chiba University, Chiba, Japan

In laser dye thermal transfer printing, high resolution and continuous tone images can be easily obtained, since a laser light focuses on a small spot, and its heat energy can be controlled by pulse width modulation. On the other hand, the physical phenomena occurring in an ink donor sheet during or just after the laser heating have not been clarified yet. In this article, the surface of the ink layer consisting of sublimation color dye is heated by microsecond laser pulse irradiation and is observed using time resolved optical microscopy. The ink layer is deformed during and after laser pulse irradiation. A small hole is formed as a result of melt and ablation of the ink layer upon laser heating. The diameter of the hole increases rapidly after passing through an induction period, but then the rate of increase slows down. A successful explanation is made of such thermal responses of the ink layer on the time scale of microseconds by assuming Gaussian spatial distribution of laser light intensity and the diffusion of the heat energy by thermal conduction.

Journal of Imaging Science and Technology 44: 484–490 (2000)

Introduction

Laser dye transfer printing (LDTP) is a color hardcopy technology which enables the formation of very high definition images.[1–4] The principle of LDTP is shown schematically in Fig. 1. The ink sheet is composed of a laser light absorbing layer and a color ink layer. The laser beam focused by a lens irradiates the laser light absorbing layer in which the light energy is converted into thermal energy, and the color dye ink layer is heated. This energy conversion process causes sublimation or melting of a dye in the ink layer and transfer of it to the receiving sheet, leading to the formation of a dye image on a receiving sheet. This LDTP method possesses several advantages:

(i) A focused laser is used as a heat source, so that the dots corresponding to the size of a laser spot (several micrometers) are printed, therefore, it becomes feasible to obtain a high image resolution of more than 2,540 dpi.

(ii) The amount of transferred dye can be controlled by varying the exposure energy of laser light, hence each dot comprising the image has a characteristic of continuous tone.

However, in spite of the technological importance of LDTP, the basic physical phenomena occurring at the ink sheet during or just after the laser heating have not been clarified yet. This is probably because the dye transfer occurs in a very small region and its time scale is very short. In the last few years, we have studied the dye transfer mechanism on the basis of the effect of laser heating on multiple layered ink donor sheets.[5,6]

In this article, we design and construct an experimental setup for time resolved optical microscopy[7,8] and conduct in situ observation of the imaging medium during laser irradiation. The time resolved microscopic observation is demonstrated using a double layered sample similar to the ink donor sheet, and the thermal response of the ink layer is observed. Transient deformations of the sample are discussed on the basis of the change in the energy density distribution of laser spot with time.

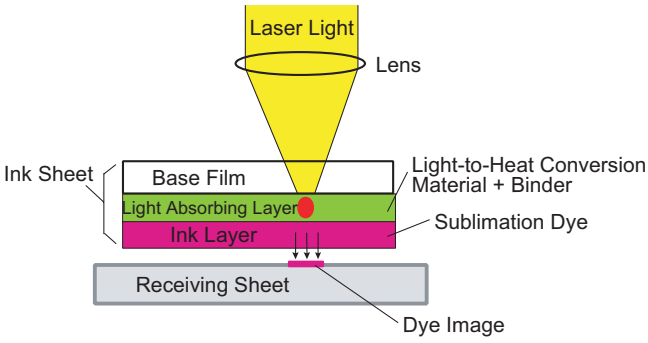

Figure 1. Principle of laser dye transfer printing.

Original manuscript received May 2, 2000

▲ IS&T Member

‡ E-mail: kinoshita@e-image.tp.chiba-u.ac.jp

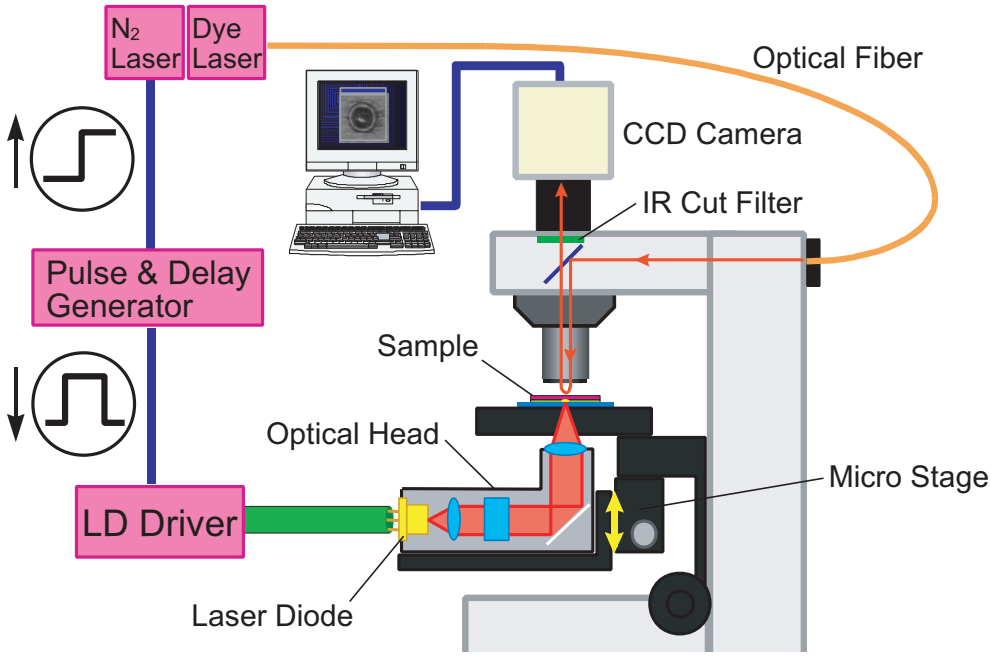

Figure 2. Schematic diagram of experimental setup for time resolved microscopy.

Experimental

Experimental Apparatus

The experimental setup using an optical microscope (Olympus Optical Co., Ltd., BX60M) is shown in Fig. 2. The construction of the apparatus is similar to the one used in Ref. 8 except for the exposure source. Test samples were placed on the stage of the microscope. The imaging optical head including a laser diode (LD, Tottori Sanyo Electric Co., Ltd., DL-8032; wavelength, 830 nm; laser power, 150 mW) was set under the sample stage. The distance between the sample and the optical head is variable, as the optical head is set on the z axis stage, and the distance can be measured using the gradations on a micrometer. Therefore, the optical spot size on the imaging medium can be controlled by a movement of the z axis stage. A nitrogen pumped dye laser (Laser Science, Inc., VSL-337 and DLM-110; pulse width 3 ns fwhm; wavelength ca. 610 nm, emitted from Rhodamine B dye) was used as an illumination source. The delay time between imaging and illumination laser pulses was controlled by a digital delay/pulse generator (Stanford Research Systems, Inc., DG535). An infrared ray (IR) cutoff filter to intercept the imaging laser pulse was set in front of a CCD camera (Fuji Photo Film Co., Ltd., HC-300).

Time resolved microscopic measurements were carried out in the following manner. Irradiation is started by sending an imaging pulse from the pulse generator to an LD driver. After a certain delay time, an illumination trigger pulse is sent to the N_2 pumped dye laser, which is connected to the reflected illumination portal of the microscope by an optical fiber, and then the surface of the sample is illuminated instantaneously with a 3 ns dye laser pulse. An observation image is captured by a CCD camera and stored in a personal computer. Because the single observation image is available for each imaging laser irradiation event, a series of time resolved images can be obtained by repeating the observation while changing the delay time and the position of sample.

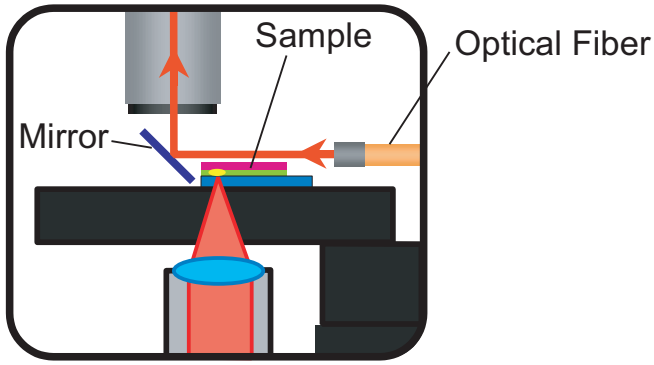

Figure 3. Schematic of experimental setup for side view observation.

As shown in Fig. 2, the surface of the sample was usually observed from above. We also observed a side view of the sample by placing a mirror on the stage and illuminating the side of the sample (Fig. 3).

Preparation of Samples

The structure of the double layered sample used for the time resolved microscopy is shown in Fig. 4. A mixture of IR absorbing dye (Mitsui Chemical Co., Ltd., PA-1006) and polycarbonate (Teijin Kasei Co., Ltd., Panlite K1300) was coated on a transparent acrylic plate by the usual spin coating method. The ratio of IR absorbing dye to polycarbonate was adjusted to 1:1 by weight. Then, a magenta sublimation dye (Mitsui Chemical Co., Ltd., MS Magenta VP) was coated on the laser light absorbing layer by vacuum evaporation. The sample is similar to a double layered ink donor sheet. The thickness of the laser light absorbing layer and the ink layer were 1.8 μm and 1.5 μm, respectively. The observations were made without a receiving sheet in order to observe the surface of the ink layer directly.

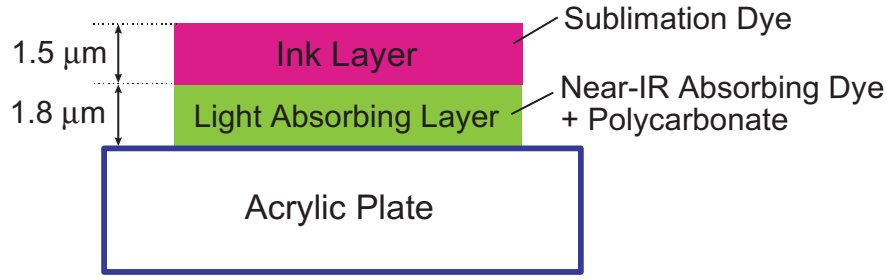

Figure 4. Structure of double layered sample.

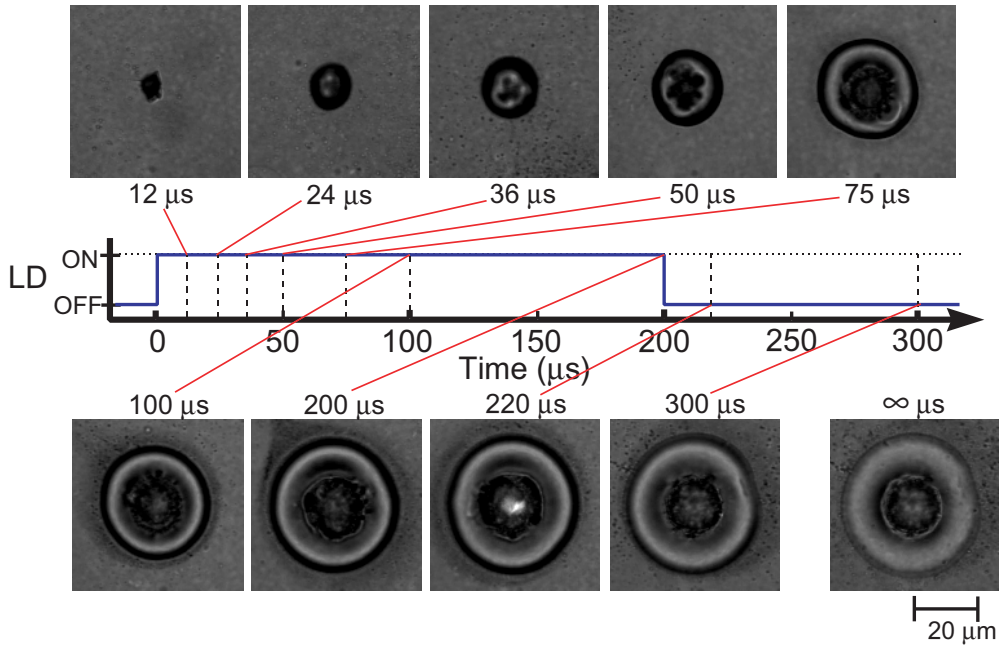

Figure 5. A series of time resolved microphotographs of ink surface. Laser power and spot size are 60 mW and 25 µm, respectively.

Results and Discussion

Time Resolved Microscopy of Ink Surface

Figure 5 shows a series of top view photographs of the ink layer recorded during and after laser pulse irradiation. The laser power and the pulse width were 60 mW and 200 µs, respectively. The optical spot size was 25 µm in diameter. The photographs, at delays from 12 µs to 200 µs are recorded during pulse irradiation and at 220 µs to 3 s are after the ceasing of irradiation. At 12 µs duration, the central region of the ink surface corresponding to the beam center begins to swell out. This physical change of the ink layer may be caused by expansion of the laser light absorbing layer and melting of magenta dye by heating. The region of swelling and melting continued to spread out circularly with heating time. At 36 µs duration, the center of the swelling region began to sink and the rim was formed at the edge of the spot. Then, the formation of a hole was observed at 75 µs duration. The diameters of the rim and the hole increase until ceasing of the laser pulse at 200 µs. Because the surface of the acrylic plate was visible at the inside region of the hole, the hole was found to be formed through the laser light absorbing layer. Within a few seconds after ceasing of laser pulse irradiation, the melting dye was solidified on cooling to room temperature, and the deformation, rim and hole, remained unaltered permanently.

Side View Observation

Figure 6 shows the time resolved images of the side view of the ink surface during and after laser pulse irradiation. At 24 µs, the expansion of the ink layer was observed at the center of the exposed spot area. The height of the expanded convex area is 4.5 µm, and the total thickness including the ink layer and the laser light absorbing layer was increased by a factor of 2.3. While the expanded region increased in width with irradiation time, the height decreased slightly and was 3.0 µm at the end of the laser pulse irradiation at 200 µs. After cooling to ambient temperature, the rim structure with a height of 2.0 µm was observed around the hole. The large expansion occurring over the initial 24 µs of the irradiation time is attributable to the effective contribution of thermal energy to the deformation, whereas hole formation may lead to the loss of the thermal energy at irradiation times beyond 24 µs. Time resolved microscopic observation of the ink layer revealed that laser heating caused expansion, spread, and contraction of the layer in several tens of microseconds. In view of the above expansion phenomena of the ink surface without pressure on the ink and receiving sheets, LDTP may be one of the promising techniques for the formation of stable and high resolution images.

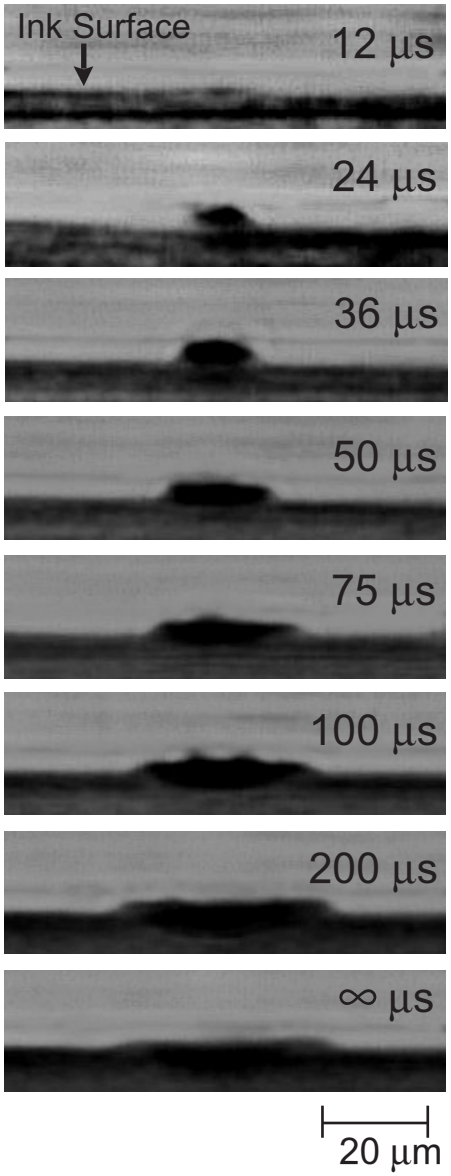

Figure 6. A series of time resolved microphotographs of sectional view of sample specimen. Laser power and spot size are 60 mW and 25 μm, respectively.

Energy Density Distribution of Laser Spot

We will concentrate on the energy density distribution of the laser spot in order to discuss the transient deformations shown in Fig. 5. As shown in Fig. 7, if we assume the energy density J of the laser spot has a Gaussian spatial distribution and increases with increasing the irradiation time t, the radial distribution of J is formulated as follows:

$$J(r) = \frac{2P \cdot t}{\pi W^2} \exp\left(-\frac{2r^2}{W^2}\right) \qquad (1)$$

where P is the laser power, r the distance in radial direction, and W the radius of the laser spot corresponding to the value of r at an energy density of $J(0)/e^2$. We assumed a threshold energy density, J_{th}, for the hole or rim formation as shown in Fig. 7. For example, assuming that J_{th} is the threshold value for hole formation, no

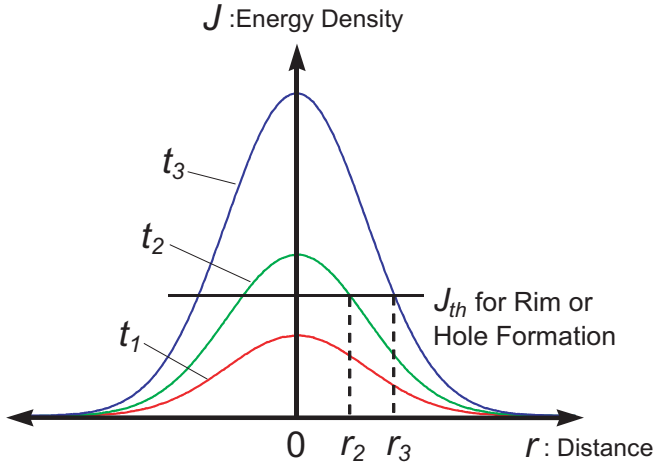

Figure 7. Distribution of energy density of laser spot. J and r axes indicate the irradiating energy density and distance in the radial direction, respectively; J_{th} is the threshold energy density for the rim or hole formation.

hole is formed at an irradiation time t_1 because the irradiation energy density at t_1 is lower than J_{th}. At time t_2, the hole of radius r_2 is formed, and at time t_3 the hole radius increases up to r_3. Thus, the rim or hole radius is a function of irradiation time t. The rim or hole radius $r(t)$ at laser irradiation time t is expressed as follows[7,8] using Eq. 1:

$$r(t) = \begin{cases} 0 & \dfrac{2 \cdot P \cdot t}{\pi W^2} < J_{th} \\ \sqrt{\dfrac{W^2}{2} \ln\left(\dfrac{2 \cdot P \cdot t}{J_{th} \cdot \pi W^2}\right)} & \dfrac{2 \cdot P \cdot t}{\pi W^2} \geq J_{th} \end{cases} \qquad (2)$$

Radii of Rim and Hole

The rim radius, which is defined as a distance between the outside edge of rim and the center of hole, and the hole radius during laser pulse irradiation were determined by using the time resolved images. Figures 8 and 9 show the irradiation time dependence of the rim and hole radii, respectively. The solid curves in the figures show the calculated values fitted to the experimental data using Eq. 2. In Figs. 8 and 9, the threshold energy densities J_{th} for the rim and hole formation were determined as 3.4×10^3 J/m^2 and 7.2×10^3 J/m^2, respectively. These values were calculated from the rising points of the curves in Figs. 8 and 9.

As shown in Fig. 8, the rim radius increases rapidly beyond the threshold time of 12 μs. The images in Fig. 5 indicate that the formation of the rim is preceded by the melting of dye in the tiny region of the beam center. The temperature of the ink surface at t = 12 μs can be calculated by an equation of thermal conduction using two dimensional cylindrical coordinates.[9] The heat generation in the equation takes into account the Gaussian laser beam that is absorbed by the laser light absorbing layer on the basis of Lambert–Beer's law. Based on calculation, we infer that a temperature as high as 120°C was attained, which corresponds to the melting point of the dye. In the case of rim formation, the data exceed the calculated curve in the latter half of the laser pulse. One of the reasons for this devia-

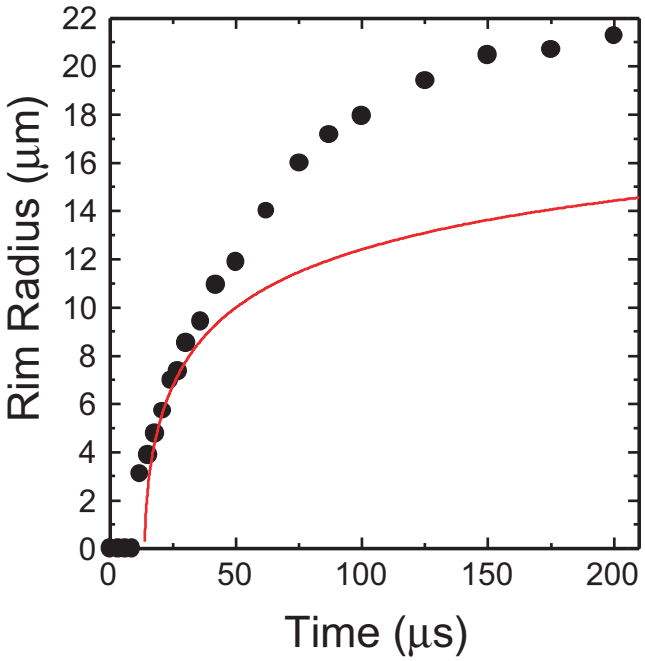

Figure 8. Plots of rim radius versus irradiation time. The curve in the figure represents calculated values fitted to the data using Eq. 2.

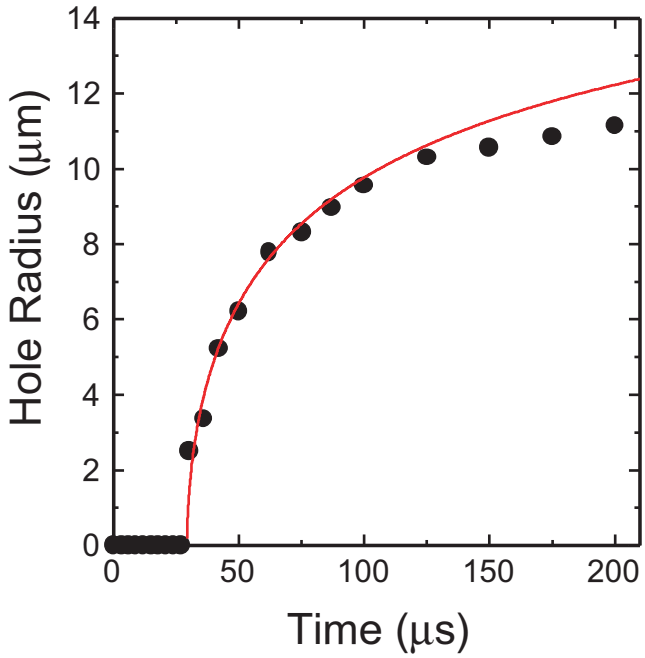

Figure 9. Plots of hole radius versus irradiation time. The curve in the figure stands for calculated values fitted to the data using Eq. 2.

tion may be due to the diffusion of energy by thermal conduction. The effect of thermal conduction is not considered in Eq. 2, but its effect on the melting of the dye on the time scale of microseconds should be required for a more reliable simulation. Another reason may be that the molten dye moves around, owing to the effect of surface tension in the liquid phase and the high pressure caused by the hole formation.

In Fig. 9, the data show a good fit to the calculated curve except for the small deviation at the latter half of the pulse (t > 125 μs). In this case of hole formation, there is a possibility that the physical events in the ink sheet occurs in a similar manner as the laser ablation transfer because the hole was also formed through the laser light absorbing layer. In general, by introducing the threshold energy in the analysis of laser ablation phenomenon,[7,10] the experimental results on hole formation can be explained well, and agreement with the calculated values obtained. In this case also, we have to take into account the effect of thermal conduction on hole formation. The agreement between the experimental (closed circle) and calculated values (solid curve) in Fig. 9 may be dependent on the balance of the thermal conduction to the acrylic base plate and thermal diffusion in the plane of the ink layer.

It was confirmed that the fundamental characteristics of thermal response of the ink sheet, namely, rapid increase in the initial stage and the subsequent slow increase in the hole radius with irradiation time, were determined by the time course of the energy density distribution on the time scale of microseconds.

Time Resolved Microscopic Observation of Light Absorbing Layer Surface

Physical events occurring in the ink layer and the laser light absorbing layer will be considered separately to further understand the hole formation in a double layered ink sheet. We prepared a sample specimen consisting only of a laser light absorbing layer that is coated on the acrylic plate (no ink layer). This further simplifies the phenomena occurring in the laser heating area. Time resolved microscopic measurements were carried out using the sample specimen.

Figure 10 shows the top view photographs of the laser light absorbing layer during and after laser pulse irradiation. The recording condition was the same as that employed for the double layered sample. As can be seen in these photographs, hole formation was also observed during the irradiation even in the absence of the ink layer. The surface temperature of the laser light absorbing layer at beam center was calculated to be 400°C at t = 12 μs.[9] Hence, it is reasonable to consider that hole formation is caused by the thermal decomposition of the laser light absorbing layer.[11]

We also measured the hole radius using time resolved images. Closed squares in Fig. 11 show the irradiation time dependence of hole radius in the light absorbing layer coated on the acrylic plate. The solid curve in the figure is the calculated values fitted to the data using Eq. 2 and the threshold value of $J_{th} = 3.3 \times 10^3$ J/m^2. Closed circles in Fig. 11 show the hole radius in the light absorbing layer coated on a glass plate, and closed triangles indicate an isolated light absorbing layer which was obtained by peeling off the layer formed on the glass plate. There were marked differences observed among the three sample specimens. This may be due to the difference in thermal conductivity among these base plates. Thermal conductivity of glass is higher than that of acrylic resin, so that it is expected that more heat energy is conducted to the glass plate than to the acrylic plate. Consequently, heat losses due to the conduction to the base plate result in less effective heating of the layer and therefore the decrease in the hole radius. In contrast, the amount of heat effusion through an ambient atmosphere is expected to be quite small

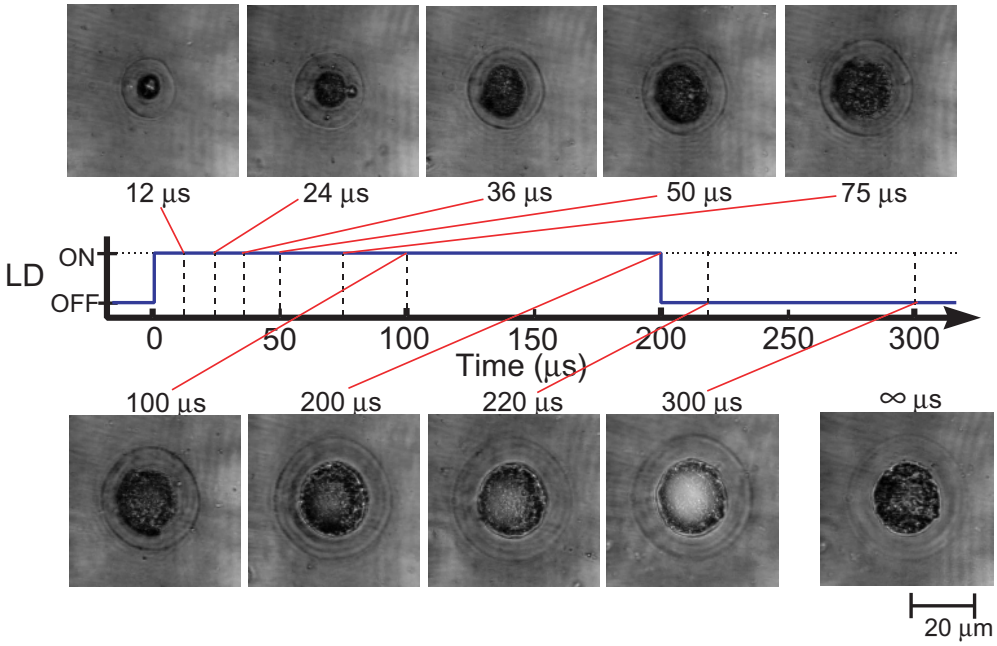

Figure 10. A series of time resolved microphotographs of light absorbing layer surface. Laser power and spot size are 60 mW and 25 µm, respectively.

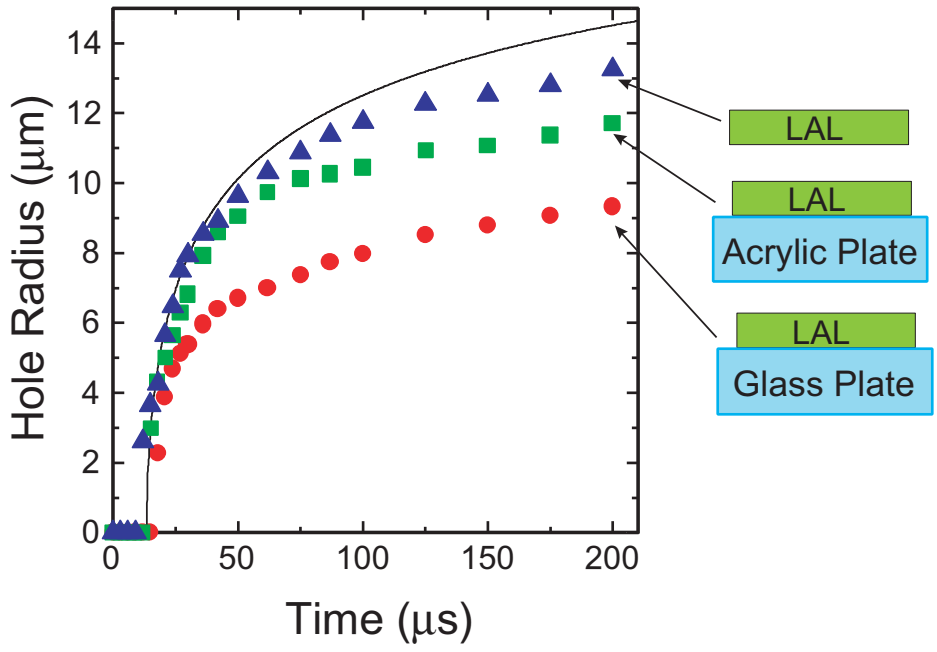

Figure 11. Plots of hole radius versus irradiation time. The smooth curve is fitted to the data using Eq. 2. Squares, circles, and triangles show measured points taken on the samples of laser light absorbing layer (LAL) on the acrylic plate, LAL on the glass plate, and LAL free standing film, respectively.

for the isolated layer film. This leads to the enhancement in the hole radius and a good agreement between the calculated and found values (see triangles in Fig. 11). These results indicate that the thermal conduction has a major role in the transient behavior of the light absorbing layer in the time scale of microseconds.

Conclusions

An experimental setup for time resolved microscopic measurements were constructed in order to investigate the dye thermal transfer mechanism of the laser dye transfer printing method. The experimental results using the double layered sample similar to an ink sheet

indicated that the rim formation due to a melting of the dye and hole formation due to a thermal decomposition like an ablation occurred during the laser pulse irradiation. These transient responses were found to be greatly affected by the variation in the distribution of energy density and the thermal properties of materials used. ▲

References

1. K. W. Hutt, I. R. Stephenson, H. C. V. Tran, A. Kaneko, and R. A. Hann, *Proceedings of IS&T's 8th International Congress on Advances in Non-Impact Printing Technologies,* IS&T, Springfield, VA, 1992, p. 367.
2. S. Sarraf, C. DeBoer, D. Haas, B. Jadrich, R. Connelly, and J. Kresock, *Proceedings of IS&T's 9th International Congress on Advances in Non-Impact Printing Technologies/Japan Hardcopy '93,* IS&T, Springfield, VA, Soc. Electrophotogr. Japan, Tokyo, Japan, 1993, p. 358.
3. N. Egashira, S. Mochizuki, Y. Aimono, and N. Lior, *J. Imaging Sci. Technol.* **37,** 167 (1993).
4. Y. Odai, M. Katoh, T. Kitamura and H. Kokado, *J. Imaging Sci. Technol.* **40,** 271 (1996).
5. T. Kitamura, M. Kinoshita and Y. Odai, *Proceedings of IS&T's 12th International Conference on Digital Printing Technologies*, IS&T, Springfield, VA, 1996, p. 258.
6. M. Kinoshita and T. Kitamura, *Proceedings of IS&T's 13th International Conference on Digital Printing Technologies*, IS&T, Springfield, VA, 1997, p. 765.
7. I.-Y. S. Lee, W. A. Tolbert, D. D. Dlott, M. M. Doxtader, D. M. Foley, D. R. Arnold, and E. W. Ellis, *J. Imaging Sci. Technol.* **36,** 180 (1992).
8. D. E. Hare, S. T. Rhea, D. D. Dlott, R. J. D'Amato, and T. E. Lewis, *J. Imaging Sci. Technol.* **41,** 291 (1997).
9. Y. Odai, M. Katoh, T. Kitamura, and H. Kokado, *Soc. J. Electrophotogr. Japan* **35,** 315 (1996) (in Japanese).
10. F. Habbal, E. B. Cargill, W. Smyth, and G. Whitesides, *Proceedings of IS&T's 12th International Conference on Digital Printing Technologies,* IS&T, Springfield, VA, 1996, p. 570.
11. M. Kinoshita and T. Kitamura, *Proceedings of IS&T's 14th International Conference on Digital Printing Technologies,* IS&T, Springfield, VA, 1998, p. 273.